Pediatric Radiology (2022) 52:1895–1909
https://doi.org/10.1007/s00247-022-05431-6

THORACIC IMAGING

Pediatric cardiothoracic vasculitis: multimodality imaging review

Evan J. Zucker[1] · **Frandics P. Chan**[1]

Received: 14 March 2022 / Revised: 19 May 2022 / Accepted: 13 June 2022 / Published online: 6 July 2022
© The Author(s), under exclusive licence to Springer-Verlag GmbH Germany, part of Springer Nature 2022

Abstract
The pediatric vasculitides are a relatively uncommon and heterogeneous group of disorders characterized by vessel inflammation, often with cardiothoracic involvement. Diagnosis and monitoring are often clinically challenging because of the nonspecific symptoms and laboratory markers. Thus, imaging has assumed increasing importance for early detection of disease activity, extent and complications as well as long-term monitoring pre- and post-treatment. Herein, we review the major pediatric vasculitides with frequent chest manifestations, including Takayasu arteritis, Kawasaki disease, granulomatosis with polyangiitis, eosinophilic granulomatosis with polyangiitis, microscopic polyangiitis, Behçet disease and potential mimics. We highlight key clinical features and management considerations, emphasizing the central role of imaging.

Keywords Children · Computed tomography · Granulomatosis · Kawasaki disease · Magnetic resonance imaging · Positron emission tomography · Takayasu arteritis · Vasculitis

Introduction

Pediatric vasculitis comprises an uncommon and often elusive spectrum of disease, broadly characterized by blood vessel inflammation in the absence of a clear cause [1, 2]. The overall annual incidence is estimated to be at least 23 per 100,000 children, with frequent cardiothoracic manifestations [1, 3]. Prompt diagnosis and recognition of disease progression remain clinically challenging because of protean symptoms ranging from early fever and malaise to later ischemic signs with multisystem end-organ involvement [1, 2]. Similarly, a variety of laboratory markers might be abnormal (such as elevated acute-phase reactants with active inflammation, or decreased renal clearance reflecting kidney tissue damage) but are usually nonspecific [1]. In addition, the disorders' phenotypic expression varies with the size of vessels involved and type of pathological vascular infiltration, among other factors [1, 4].

As such, imaging has become essential in evaluating pediatric vasculitis, facilitating earlier diagnosis and more accurate long-term monitoring. Pre-treatment, it provides a precise depiction of disease burden and a roadmap for invasive intervention if indicated. Post-treatment, it allows for ready assessment of disease activity and any complicating features [1, 2]. Although echocardiography can be helpful for initial screening of cardiovascular complications, cross-sectional imaging is often required for more detailed characterization. Herein, we present the broad application of imaging in cardiothoracic-predominant pediatric vasculitis patients, focusing on CT, MRI and positron emission tomography (PET). First we summarize disease classification schemes and multimodality imaging techniques, following with a review of the major disorders and their imitators. While highlighting pertinent clinical features and treatment approaches, we emphasize the central role of imaging.

Classification of disease

Categorization of vasculitis has been a longstanding conundrum because of the heterogeneity and rarity of the disease, a problem even more pronounced in children [5]. The most frequently used classification scheme specific to children was developed in 2005 by the European League Against Rheumatism (EULAR)/Paediatric Rheumatology European Society (PRES) [1, 2, 5, 6]. After the 2008 Ankara Consensus Conference, diagnostic standards for specific pediatric vasculitides were revised in conjunction with the Paediatric Rheumatology International Trials Organisation (PRINTO)

✉ Evan J. Zucker
zucker@post.harvard.edu

[1] Department of Radiology, Stanford University School of Medicine, 725 Welch Road, Stanford, CA 94305, USA

[7, 8]. Thus came the final EULAR/PRES/PRINTO criteria, although the overall grouping of disorders remained unchanged from the original EULAR/PRES guidance [5–8]. More recently, the often-referenced 2012 revised International Chapel Hill Consensus Conference (CHCC2012) vasculitis criteria were released, although these criteria used only adult data [4, 9].

Regardless, the EULAR/PRES/PRINTO and CHCC2012 classification schemes are largely similar, separating disorders according to the size of predominant vessel involvement [1, 2, 5–9]. Vessel sizes are denoted as large (the aorta and its major branches), medium (main visceral arteries and initial branches) or small (intraparenchymal arteries, arterioles and capillaries). EULAR/PRES/PRINTO subcategorizes the small vessel vasculitides based on the presence or absence of granulomas, whereas CHCC2012 subdivides them based on antineutrophil cytoplasmic antibody (ANCA) versus immune complex positivity [1, 6–9]. In addition, there are some differences in regard to the grouping of vasculitis associated with a secondary cause, and only CHCC2012 includes "variable vessel" and "single-organ" distinctions [5, 9].

A summary of the major pediatric vasculitides with characteristic chest involvement is presented in Table 1 according to EULAR/PRES/PRINTO groupings, with pertinent elements from CHCC2012 [6–9]. For consistency, we use EULAR/PRES/PRINTO designations henceforth throughout this text. Ultimately, it is important to acknowledge that vasculitides can affect vessels larger or smaller than their typical predilections, thus compounding difficulties in diagnosis [9].

Imaging approach

Overall, CT, MRI and [F-18]2-fluoro-2-deoxyglucose (^{18}F-FDG) PET (combined with CT or MRI) are the most high-yield imaging modalities. Radiography is usually of limited diagnostic utility beyond excluding acute complications. Ultrasound (US), including echocardiography, can be a helpful cardiovascular screening test but can underestimate or incompletely characterize the full extent of disease. Conventional angiography is preferably reserved for concurrent intervention [10, 11]. In general, the purpose of imaging in medium- to large-vessel vasculitis is to evaluate the vessels, while the goal in small- to medium-vessel vasculitis is to assess for end-organ disease complications.

Table 1 Classification of pediatric vasculitis with frequent cardiothoracic involvement

Category[a]	Major vasculitides	Chest predilection
Large-vessel[b]	Giant cell arteritis Takayasu arteritis	Takayasu arteritis
Medium-vessel[c]	Cutaneous polyarteritis Kawasaki disease Polyarteritis nodosa (PAN)	Kawasaki disease Infantile PAN
Small-vessel[d] granulomatous	Granulomatosis with polyangiitis (GPA; formerly Wegener)[e] Eosinophilic GPA (or Churg–Strauss)[e]	All disorders
Small-vessel[d] non-granulomatous	Anti-C1q vasculitis Anti-glomerular basement membrane disease Cryoglobulinemic vasculitis Henoch–Schönlein purpura Hypocomplementemic urticarial vasculitis Isolated cutaneous leukocytoclastic vasculitis Microscopic polyangiitis[e]	Microscopic polyangiitis
Other	Behçet disease (variable vessel[f]) Cogan syndrome Connective-tissue disease associated Isolated central nervous system vasculitis Secondary to infection/malignancy/drugs Unclassified	All except Cogan syndrome and isolated central nervous system

[a]Adapted primarily from the European League Against Rheumatism (EULAR)/Paediatric Rheumatology European Society (PRES)/Paediatric Rheumatology International Trials Organisation (PRINTO) criteria [6–8] with selected descriptors from the 2012 revised International Chapel Hill Consensus Conference (CHCC2012) criteria [9]

[b]Predominance for aorta and major branches

[c]Predominance for main visceral arteries and initial branches

[d]Predominance for intraparenchymal arteries, arterioles, capillaries

[e]Antineutrophil cytoplasmic antibody (ANCA) positive

[f]No predilection; may affect any size and type of vessel

The choice of CT, MRI or hybrid PET/CT or PET/MRI depends on the specific disorder, patient factors, clinical preferences and institutional technical capabilities. CT is generally more optimal for assessing the lungs, airways and coronaries as well as any calcifications (e.g., from chronic inflammation) or metallic material (e.g., post-surgical stents). MRI offers improved tissue (e.g., vessel wall) characterization and nearly comparable spatial resolution without ionizing radiation and potentially without contrast agent [1, 2, 10, 11]. Nevertheless, these traditional distinctions have become increasingly blurred with ongoing advances both in CT (e.g., dual-energy/spectral CT for improved tissue contrast; CT-derived fractional flow reserve for coronary stenosis hemodynamic interrogation) and MRI (e.g., ultrashort echo time [UTE] and zero echo time [ZTE] techniques with conical or radial k-space sampling for lung and airway assessment; four-dimensional [4-D] blood-flow interrogation) [12–16]. ^{18}F-FDG PET provides a surrogate for disease activity in resolvable vessels (>4 mm) and non-vascular end-organ sites, which can be quantified via the standardized uptake value (SUV) [1, 2, 17]. However, there are no specific SUV cutoffs for disease, and radiotracer uptake does not consistently predict progression [18]. In the end, given the heterogeneity and chronicity of pediatric vasculitis and overall lack of well-established guidelines, the decision to pursue imaging or select a particular modality must be individually tailored to balance expected gains with any potential harms/drawbacks (e.g., ionizing radiation, contrast agent or sedation exposure, discomfort, cost) while also considering local technical expertise and resources [18, 19].

Large-vessel vasculitis: Takayasu arteritis

Takayasu arteritis is typified by granulomatous inflammation, possibly autoimmune in nature, of predominantly the aorta and its major branches [1, 2, 5–9]. Arterial wall inflammation leads to concentric wall thickening and fibrosis with subsequent stenosis, occlusion and less commonly aneurysm formation, which is sometimes accompanied by mural thrombus [1, 2]. Six types exist based on the pattern of disease: Type I, supra-aortic arteries; Type IIa, ascending aorta or arch only; Type IIb, descending aorta with or without proximal aorta and arch; Type III, arch and branches plus descending and abdominal aorta or renal arteries; Type IV, abdominal aorta or renal arteries only; and Type V, generalized involvement, including features of other types [2].

While Takayasu arteritis is rare, with an estimated childhood incidence of 0.4–6.3 cases per million, it is in fact the third most common pediatric vasculitis and the most frequent large-vessel vasculitis affecting children and young adults [1, 20]. Asian women ages 20–40 are the most typically affected demographic, although Takayasu arteritis has been reported in children as young as 6 months [1, 21]. In addition to Asia, the disease is more common in South America and the Mediterranean region than elsewhere in the world [20, 21]. Symptoms vary with the stage of disease, ranging from nonspecific constitutional fatigue and fever with active inflammation to the classic "pulseless" phase with vascular steno-occlusion [1]. The EULAR/PRES/PRINTO criteria require an angiographic abnormality plus at least one of the following: pulse deficit or claudication, blood pressure discrepancy, bruit, hypertension or elevated acute phase reactants [2, 21]. Corticosteroids are the first-line treatment and can be augmented with biologic agents or immunosuppressants for resistant disease or steroid-associated complications. Surgical and endovascular repair are second-line options, the former associated with better long-term outcomes although it is more invasive [22].

Both CT and MRI can adequately show the mandatory angiographic abnormalities required for diagnosis and also enable long-term follow-up [1]. Early CT findings include arterial wall thickening with mural enhancement and a low-attenuation ring-like appearance on delayed acquisitions (Fig. 1). Later findings include less pronounced wall thickening containing areas of high attenuation or calcification, along with arterial steno-occlusion or aneurysm formation [1, 2, 18].

Magnetic resonance imaging offers better characterization of the vessel wall inflammation, in addition to angiographic evaluation [1, 2]. Table 2 provides a sample MRI protocol for thoracic involvement of large-vessel vasculitis/Takayasu arteritis [23]. Fat-suppressed T2-weighted imaging allows for assessment for wall edema, which in one adult cohort was found in 94% of Takayasu arteritis patients with definite active disease but also in 56% with seeming clinical remission (Fig. 2) [24]. T1-weighted sequences pre- and post- intravenous (IV) gadolinium contrast administration permit evaluation for wall enhancement (relative to myocardium), which was found to be 88.5% concordant with clinically active disease in a small group of Takayasu arteritis patients [25]. T1 black-blood images are preferred to gradient-echo technique if feasible for their greater conspicuity of the enhancing wall [1]. Late gadolinium enhancement (e.g., 10–15 min post contrast administration) might improve disease detection; however, late gadolinium enhancement can be appreciated in both active disease and chronic fibrosis and thus is a less helpful differentiator (Fig. 3) [26].

Although not widely used, low b value (50 s/mm^2) diffusion-weighted imaging (DWI) MRI was comparable to late gadolinium enhancement but superior to T2 for demonstrating apparent vessel wall inflammation and thus might be a useful non-contrast adjunct [27]. In one study, late vessel wall enhancement after IV administration of the blood-pool gadolinium contrast gadofosveset (rather than a typical

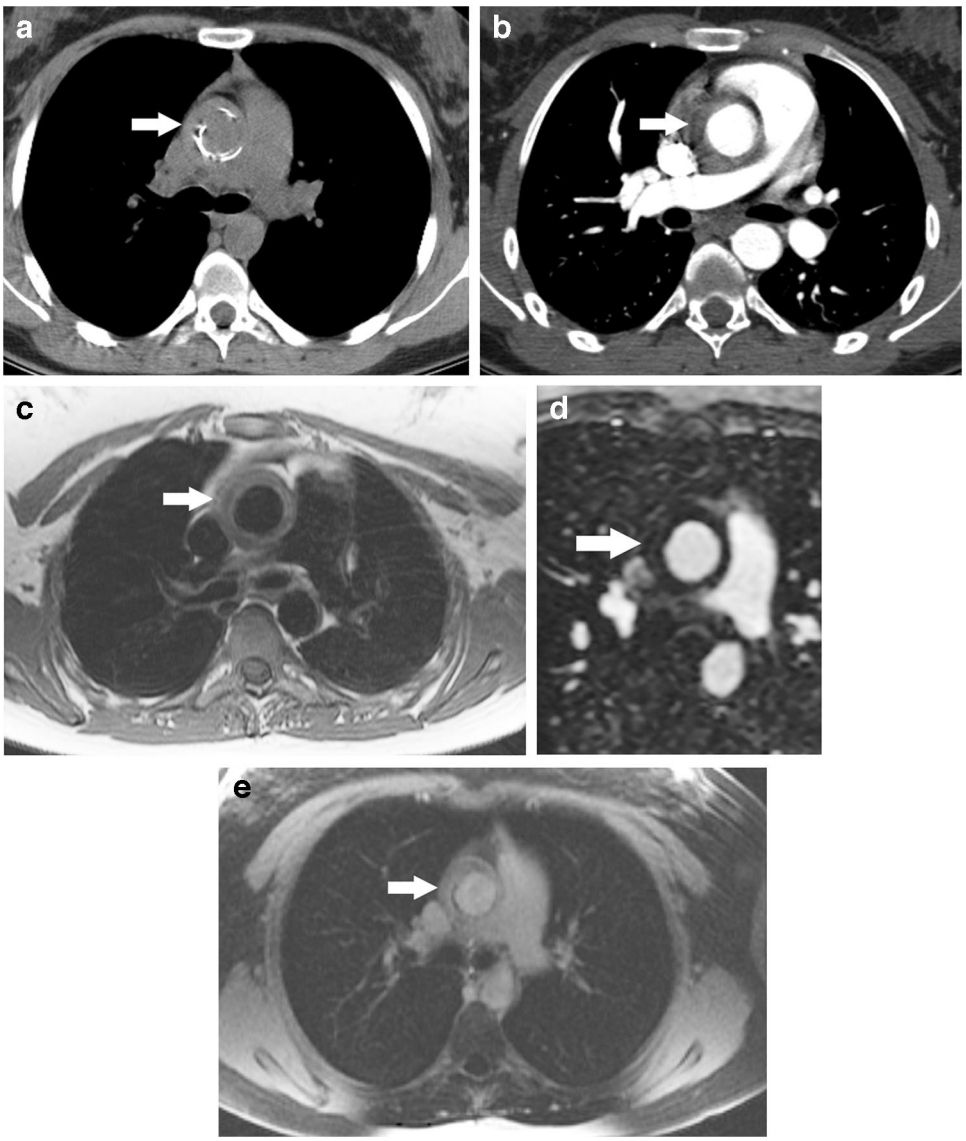

Fig. 1 Takayasu arteritis in an 18-year-old woman. **a, b** Axial non-contrast (**a**) and contrast-enhanced (**b**) chest CT angiograms show marked wall thickening of the ascending aorta (*arrow*), with associated calcification. **c** Axial T1-weighted black-blood MR image confirms the marked ascending aortic wall thickening (*arrow*). **d** Axial reformatted image from a gadolinium-enhanced MR angiogram (same exam) using T1-weighted spoiled gradient echo (SPGR) technique again shows the ascending aortic wall thickening (*arrow*) without significant luminal narrowing. **e** Axial delayed gadolinium-enhanced T1-weighted fat-saturated SPGR MR image shows enhancement of the thickened aortic wall (*arrow*), consistent with active inflammation

extracellular agent) was found to be highly accurate (100% sensitive, 89% specific) for differentiating active vs. inactive disease based on clinical criteria [28]. Unfortunately, gadofosveset is no longer obtainable in the United States or Europe because of insufficient market demand, and no other gadolinium-based intravascular contrast agent is available

Table 2 Representative thoracic MRI protocol for large-vessel vasculitis/Takayasu arteritis

Sequence	Plane	Purpose
Dark-blood T2 FS TSE	Axial	Arterial wall thickness and edema
DWI (optional)	Axial	Arterial wall diffusion restriction
Pre-contrast 3-D T1 FS SPGR	Axial	Baseline for post-contrast
CE-MRA (3-D T1 SPGR)	Coronal	Arterial stenosis and dilation
Early (1 min) post-contrast 3-D T1 FS SPGR	Axial	Early wall enhancement
4-D Flow (optional)	Axial	Arterial flow and velocity
Delayed (15 min) post-contrast 3-D T1 FS SPGR	Axial	Delayed wall enhancement

Adapted from protocol described in [23]. Field-of-view can be extended to whole body if indicated

3-D three-dimensional, *4-D* four-dimensional, *CE-MRA* contrast-enhanced magnetic resonance angiography, *DWI* diffusion-weighted imaging, *FS* fat-saturated, *MRI* magnetic resonance imaging, *SPGR* spoiled gradient echo, *TSE* turbo spin echo

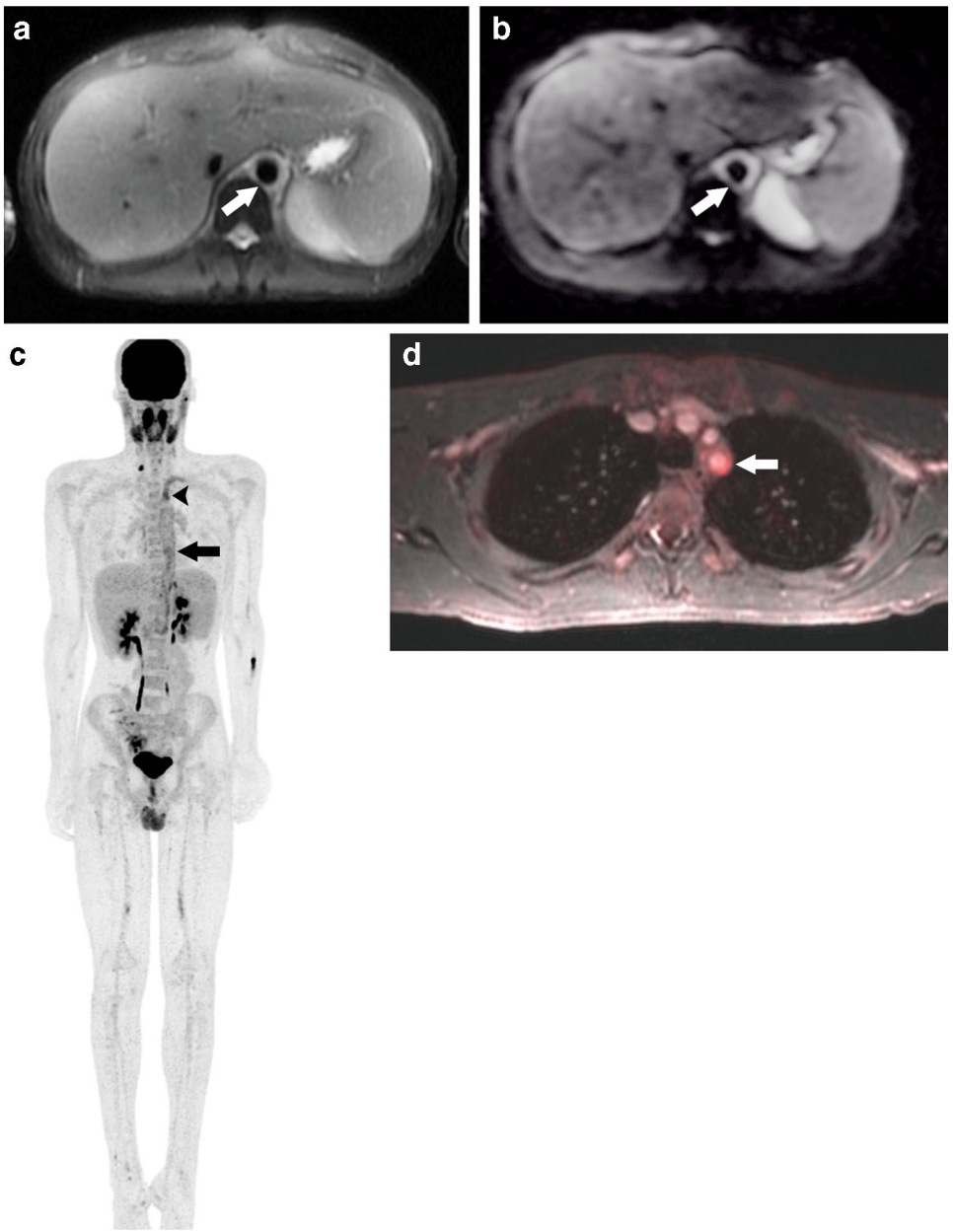

Fig. 2 Takayasu arteritis in a 15-year-old boy with active disease. **a, b** Axial T2-weighted fat-saturated (**a**) and diffusion-weighted (**b**) MR images show increased signal in the thickened wall (*arrow*) of the upper abdominal aorta, suggesting active inflammation. **c** Whole-body coronal maximum-intensity projection (MIP) image from an [F-18]2-fluoro-2-deoxyglucose (^{18}F-FDG) positron emission tomography (PET)/MRI shows diffuse uptake throughout the descending aorta (*arrow*), with more intense focal uptake in the left subclavian artery (*arrowhead*), consistent with active disease. **d** Axial fused PET/T1-weighted gadolinium-enhanced spoiled gradient echo MR image confirms focal radiotracer uptake in the thickened wall of the left subclavian artery origin (*arrow*)

[29]. As such, interest has grown in using the ultrasmall superparamagnetic iron oxide agent ferumoxytol as an off-label vascular contrast agent [30]. Recent preliminary data have suggested a link between increased aortic wall ferumoxytol uptake (decreased T2* signal) and aortic wall inflammation, likely related to phagocytic activity, although this phenomenon has not been specifically evaluated in Takayasu or other vasculitides [31].

^{18}F-FDG PET, which can be co-registered with CT or MRI, provides further complementary information on disease activity, evidenced by vessel wall radiotracer uptake, usually in a smooth and linear pattern [1, 2, 18]. The degree of FDG avidity can be scored in a semiquantitative fashion (0=none, 1 = less than liver, 2 = similar to liver, 3 = more than liver) or quantified by the maximum standardized uptake value [18]. A maximum SUV of 1.3 was proposed as a threshold for active disease, but the literature is inconsistent on the optimal value [2, 18]. In one meta-analysis, FDG PET was reported to have only moderate accuracy (sensitivity, 87%; specificity, 73%) for identifying clinically active disease; however, this study did not account for the potentially increased diagnostic accuracy from a simultaneous CT or MRI acquisition [32].

Positron emission tomography can be especially helpful in atypical cases because Takayasu arteritis is often a diagnosis of exclusion. Nevertheless, its role in disease

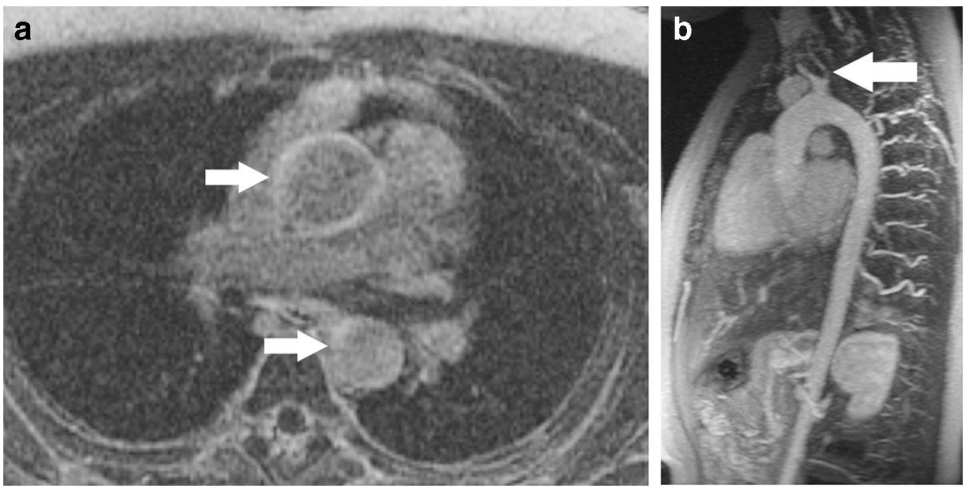

Fig. 3 Takayasu arteritis in a 9-year-old girl with late gadolinium enhancement. **a** Axial MR image obtained using magnitude inversion recovery technique and a spoiled gradient echo readout shows abnormal late gadolinium enhancement in the ascending and descending aortic walls (*arrows*), a finding that can be caused by vascular inflammation or fibrosis. **b** Sagittal maximum-intensity projection (MIP)-reformatted image from a contrast-enhanced MR angiogram shows an incidental common origin of the brachiocephalic and left common carotid arteries. There is irregular narrowing in the proximal left common carotid artery (*arrow*), in keeping with steno-occlusive Takayasu disease. The left subclavian artery was non-visualized and occluded

prognostication is less clear. For example, FDG uptake does not consistently correlate with inflammatory markers; indeed, it can decrease or normalize with treatment but also remain persistent despite apparent clinical remission [18]. Ultimately, PET/CT might be considered an excessive radiation burden in the pediatric Takayasu patient for the information obtained, or too unwieldy to perform if MRI is also needed. However, hybrid PET/MRI has recently emerged as a promising one-stop tool for Takayasu arteritis, facilitating in one exam a whole-body assessment of anatomical (e.g., luminal stenosis), morphological (e.g., wall thickening and edema) and physiological (e.g., FDG avidity) disease activity [33]. Still, experience with PET/MRI in pediatric Takayasu arteritis is limited, and continued study is likely prudent.

Medium-vessel vasculitis: Kawasaki disease

Kawasaki disease, also known as mucocutaneous lymph node syndrome, is a systemic inflammatory disease affecting medium-size as well as small vessels throughout the body with characteristic coronary involvement [1, 2, 34]. The etiology remains unclear, but the disorder is postulated to be triggered by an unknown source, possibly an infectious pathogen, which leads to downstream inflammatory incitement of the immune system [34]. Although rare, with an estimated incidence 20.8 per 100,000 children younger than 5 years in the United States, Kawasaki disease is in fact the second most common pediatric vasculitis and the most common cause of acquired cardiac disease in children [1]. It has a predominance in boys ages 6 months to 4 years of East Asian/Pacific Islander descent [1, 2, 34].

The EULAR/PRES/PRINTO and American Heart Association (AHA) diagnostic criteria for Kawasaki disease require the presence of fever for at least 5 days plus four of the five following features: mucosal changes (e.g., "strawberry tongue" erythema), conjunctivitis, polymorphous rash, extremity changes (hand/ft erythema/edema initially with later periungual desquamation) and cervical lymphadenopathy [1, 2, 6, 34]. However, fewer than four ancillary criteria are considered adequate in the presence of coronary artery involvement, although the exact number remains undefined [2, 6]. Moreover, even if full criteria are not met, a diagnosis of "incomplete" Kawasaki disease can still be entertained [34].

Kawasaki disease is not static and classically presents with 1–2 weeks of high fever (acute phase), followed by 4 weeks of continued symptoms (e.g., desquamation) but fever resolution (subacute phase), and finally 4 weeks of an asymptomatic convalescent phase [1, 2, 34]. Coronary aneurysm development is most likely to occur during the subacute phase and to a lesser extent the convalescent phase [34]. Other arterial beds can also be involved, such as the celiac, mesenteric, renal, iliofemoral and proximal upper limb arteries, with aneurysms or stenosis [2]. Of note, Kawasaki disease usually manifests differently in infants, with prolonged fever but absence of other typical clinical features, multiple arterial bed rather than isolated coronary involvement, and potentially peripheral gangrene. The spectrum of

abnormalities is termed atypical Kawasaki disease or infantile polyarteritis nodosa (PAN), another medium-vessel vasculitis that cannot be readily distinguished from Kawasaki disease given the unusual presentation at young age [1].

A major differential for Kawasaki disease is the recently described multisystem inflammatory syndrome in children (MIS-C), which presents with a Kawasaki-like illness within 4 weeks of exposure to severe acute respiratory syndrome coronavirus 2 (SARS-CoV-2), which causes coronavirus disease 2019 (COVID-19) [35, 36]. In the majority of MIS-C cases, four or more organ systems are involved (most commonly gastrointestinal, cardiovascular, dermatologic, mucocutaneous and respiratory). Approximately 2 in 5 children demonstrate fever for 5 or more days and either 4–5 Kawasaki-like clinical features or 2–3 Kawasaki-like manifestations, along with laboratory abnormalities or echocardiographic manifestations such as pericardial effusion, depressed ventricular function or coronary aneurysms, typically involving the left anterior descending or right coronaries [35]. Of note, children with MIS-C tend to be older than 5 years and more often of Afro-Caribbean descent rather than Japanese or Chinese descent, in contrast to the demographics observed in Kawasaki disease [34, 35]. At the present time, both Kawasaki disease and Kawasaki-like MIS-C are managed similarly, with intravenous immunoglobulin (Ig) and moderate- to high-dose aspirin being the first-line treatments and potential adjuncts including corticosteroids as well as tumor necrosis factor, interleukin (IL)-1, and calcineurin inhibitors and other immunosuppressive agents [34–36]. Percutaneous coronary intervention and coronary artery bypass grafting are reserved for severe coronary disease, although with potentially improved outcomes [37].

Echocardiography is recommended routinely by the AHA for suspected or known Kawasaki disease, helping to identify myocardial dysfunction and pericardial effusion during the acute phase and, most important, proximal coronary artery aneurysms during the subacute or convalescent phases, with reported high sensitivity and specificity [38]. Coronary aneurysms should be measured and categorized by size, which confers greater risk of thrombosis and infarction [1]. Both absolute measurements and z-scores relative to afebrile healthy children have been variably used for such classification purposes [38]. Suggested hybrid criteria include: normal, z-score <2; dilation, z-score 2 to <2.5 or a decrease ≥1 if initially <2; small aneurysm, z-score ≥2.5 to <5 and absolute dimension <5 mm; medium aneurysm, z-score ≥5 to <10 and absolute dimension 5 to <8 mm; and large/giant aneurysm, z-score ≥10 or absolute dimension ≥8 mm [1, 38]. In MIS-C, coronary aneurysms are less frequent and tend to be smaller than in Kawasaki disease, while left ventricular dysfunction is more common [39].

Although not formally incorporated into AHA Kawasaki disease guidelines, both CT angiography and MR angiography offer superior evaluation of the coronaries, particularly for more distal branches in older children with limited acoustic windows, as well as involvement of other vascular territories, and thus in practice are not uncommonly performed [1, 2]. PET is likely to be of less value for assessing coronary inflammation, specifically given the confounding normal physiological activity in the myocardium [2]. In general, with the latest generation dual-source scanners, CT angiography is more accurate and reliable than MR angiography for coronary assessment and might demonstrate additional aneurysms or upsize aneurysms, potentially altering management decisions (Fig. 4) [1, 40]. CT angiography also offers improved visualization of coronary calcifications and thrombus [1, 2, 40].

Nevertheless, with reported 60–80% accuracy, coronary MR angiography is still a desirable alternative without ionizing radiation and the need for an IV line and contrast

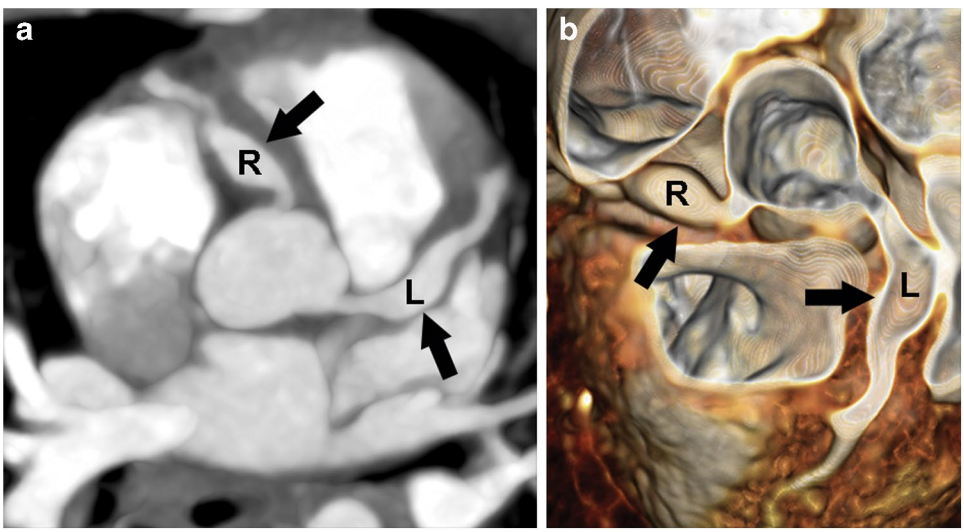

Fig. 4 CT angiography in a 5-month-old girl with Kawasaki disease. **a, b** Axial oblique maximum-intensity projection (MIP)-reformatted image (**a**) and three-dimensional (3-D) volume-rendered image oriented through the aortic root (**b**) from a contrast-enhanced electrocardiographic (ECG)-gated coronary CT angiogram show diffuse coronary dilation with fusiform aneurysms (*arrows*) of both the right coronary artery (*R*) and left main coronary artery (*L*)

material, although contrast agent can improve the signal-to-noise ratio [1, 2, 41]. Moreover, coronary MR angiography is typically performed using a 3-D electrocardiography (ECG)-triggered, navigator-gated steady-state free precession (SSFP) sequence, which is a free-breathing technique, an advantage over the breath-holding usually required for ECG-gated (or triggered) CT angiography (Fig. 5) [41]. Still, the longer imaging time and lower spatial resolution of coronary MR angiography compared to CT angiography can sometimes be problematic, particularly in young children [1, 41].

Given their coronary involvement, Kawasaki patients are also prone to myocardial ischemia and infarction, which can be assessed with stress perfusion and late-contrast-enhancement acquisitions, respectively, along with functional (cine) imaging, optimally with MRI [2]. Thus, MRI can be an even more attractive option because a single study can provide a comprehensive assessment of the coronaries (3-D SSFP), function (cine SSFP), myocardial perfusion (fast single-shot T1-weighted gradient echo post contrast and stress agent), and myocardial scar (late gadolinium enhancement) (Fig. 6) [2, 42]. Table 3 presents such a protocol [43]. While clinical guidance is inconsistent, such an examination might be most appropriate in adolescents and adults with a history of unresolved coronary aneurysm and no sedation requirements [42].

Despite providing inherently less soft-tissue contrast compared to MRI, CT can provide comparable accuracy for detecting myocardial ischemia and infarction using CT perfusion and late-iodine-enhancement acquisitions, respectively, which can be augmented with dual-energy/spectral techniques [44, 45]. Thus, CT could provide a similarly comprehensive evaluation, albeit with greater radiation burden and less Kawasaki disease–specific experience. Although not validated in Kawasaki disease, CT-derived fractional flow reserve also has potential to confirm hemodynamically

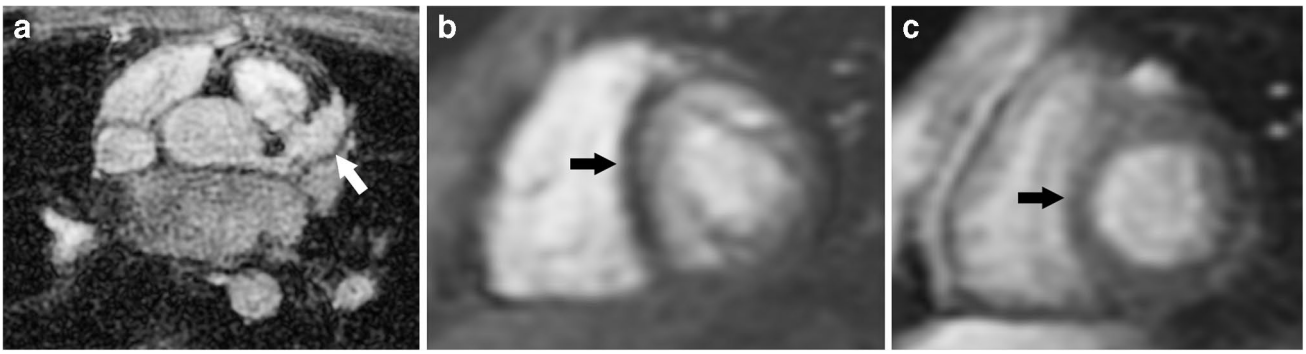

Fig. 5 MR angiography in an 11-year-old boy with Kawasaki disease. **a** Oblique axial-reformatted image from a three-dimensional (3-D) steady-state free precession (SSFP) MRI acquisition shows a large fusiform aneurysm (*arrow*) of the left anterior descending (LAD) coronary artery. **b** Short-axis gadolinium-enhanced first-pass perfusion MR image after administration of a stress agent (intravenous adenosine) shows hypointense signal in the septum (*arrow*), indicating a perfusion defect. **c** Repeat short-axis first-pass perfusion at rest shows normal perfusion of the septum (*arrow*). These findings overall suggest inducible ischemia in the septum, which is typically supplied by the LAD territory

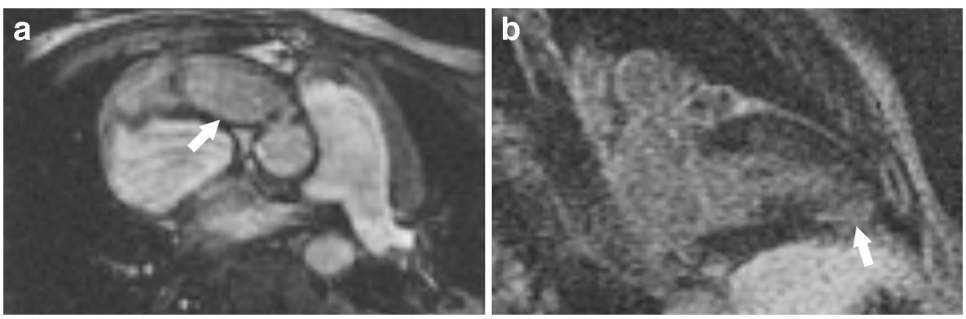

Fig. 6 Kawasaki disease in a 2-year-old girl with myocardial scar. **a** Oblique axial-reformatted image from a three-dimensional (3-D) steady-state free precession (SSFP) MRI acquisition shows a large fusiform aneurysm (*arrow*) of the right coronary artery. **b** Left-ventricular two-chamber late-gadolinium-enhancement MR image obtained using magnitude inversion recovery technique and a spoiled gradient echo readout shows abnormal infero-apical subendocardial late gadolinium enhancement (*arrow*), indicative of myocardial scar

Table 3 Representative cardiovascular MRI protocol for Kawasaki disease

Sequence	Plane	Purpose
Whole-heart 3-D SSFP (free-breathing, respiratory navigator and ECG-gated)	Axial	Coronary MR angiography (non-contrast)
2-D SSFP (breath-held, ECG-gated)	LV 2-chamber LV 3-chamber 4-chamber Short-axis	Ventricular regional wall motion, global function, and volumetry
2-D SPGR (free-breathing, ECG-gated) • Immediately after administration of stress agent (e.g., adenosine 1 mg/kg) • During contrast infusion (gadolinium 0.1 mmol/kg)	Short-axis (3–5 selected slices)	Myocardial stress first-pass perfusion
2-D PSIR-GRE (breath-held, ECG-gated)	LV 2-chamber LV 3-chamber 4-chamber Short-axis	Late gadolinium enhancement for myocardial scar/fibrosis
2-D SPGR (free-breathing, ECG-gated) • During additional contrast infusion (gadolinium 0.1 mmol/kg)	Short-axis (3–5 selected slices)	Resting first-pass perfusion

Adapted primarily from protocol described in [43]. Modifications might include omission of stress imaging if not clinically indicated and addition of post-contrast MR angiography for evaluation of extracardiac vasculature (e.g., in the chest or whole body)

2-D two-dimensional, *3-D* three-dimensional, *ECG* electrocardiogram, *GRE* gradient (recalled) echo, *kg* kilogram, *LV* left ventricular, *mg* milligram, *mmol* millimolar, *MRI* magnetic resonance imaging, *PSIR* phase-sensitive inversion recovery, *SPGR* spoiled gradient echo, *SSFP* steady-state free precession

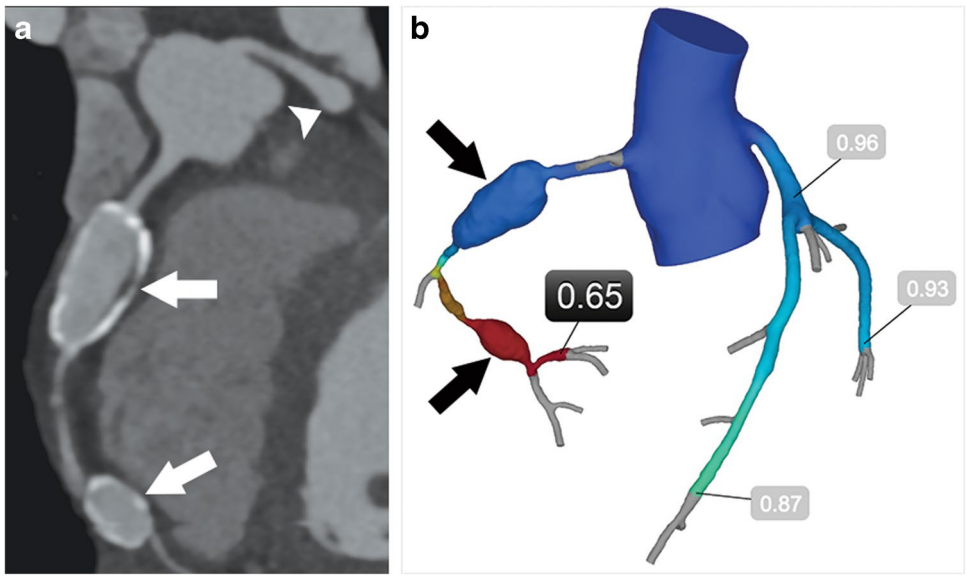

Fig. 7 Computed tomography–derived fractional flow reserve imaging in a 10-year-old boy with Kawasaki disease. **a** Curved planar-reformatted image from a contrast-enhanced, electrocardiographic (ECG)-gated coronary CT angiogram shows serial aneurysms (*arrows*) with peripheral calcification and minimal thrombus in the right coronary artery (RCA). In addition, note the smaller fusiform aneurysm (*arrowhead*) of the left main coronary artery. **b** CT-derived fractional flow reserve (FFR_{CT}) analysis post-processed from the same coronary CT angiography acquisition confirms the multiple aneurysms (*arrows*). In addition, tandem stenoses in the RCA have resulted in a distal RCA FFR_{CT} value of 0.65, which is below the 0.80 threshold and suggests hemodynamic significance. In contrast, all FFR_{CT} values in the left coronary system remain above 0.80, indicating no hemodynamic compromise

significant stenoses from existing coronary CT angiography acquisitions without the need for additional stress perfusion imaging (Fig. 7). This technique represents a physiological simulation of coronary flow, allowing for a noninvasive estimation of fractional flow reserve (FFR). FFR, previously only measurable during cardiac catheterization, is

considered the reference standard for determining the hemodynamic significance of a coronary stenosis and represents the ratio of maximal myocardial blood flow distal to a stenosis compared to the purported normal maximal myocardial blood flow in the undiseased vessel. FFR values, measured 2 cm distal to a stenosis, are considered abnormal when ≤0.80 [46].

Small-vessel vasculitis

The role of imaging in small-vessel vasculitis is to evaluate for end-organ damage. Thus, the most appropriate imaging modality and protocol depend on the organs (rather than vessels) typically involved in the disease process. Next we describe select small-vessel vasculitides with frequent cardiothoracic sequelae: granulomatosis with polyangiitis, eosinophilic granulomatosis with polyangiitis, and microscopic polyangiitis.

Granulomatosis with polyangiitis

Granulomatosis with polyangiitis (GPA), formerly known as Wegener granulomatosis, is a necrotizing granulomatous and usually ANCA-positive (and also cytoplasmic-ANCA/proteinase-3 positive) vasculitis that affects small- to medium-size muscular arteries with a predilection for airway, lung and renal involvement [1, 2, 5–8]. Coronary artery aneurysms are exceedingly uncommon but have been described in case reports [47]. The pathogenesis remains unknown, although histologically the disease is characterized by pauci-immune inflammation and fibrinoid necrosis of vessel walls [1]. Overall, GPA is rare in children, with an estimated incidence of 1 per million, more commonly affecting females (unlike its adult counterpart), with a mean age onset of 14 years [1, 5]. Symptoms are usually nonspecific (e.g., fever, malaise) but later might be attributed to end-organ lung, ear/nose/throat, or renal disease, often with multi-organ involvement [1]. Of note, airway involvement including subglottic stenosis is more common in children than in adults with GPA and is sometimes the primary presentation [48]. The EULAR/PRES/PRINTO classification requires at least three of the following criteria: histopathological evidence of arterial wall or peri-/extravascular granulomatous inflammation, upper airway (sinonasal) involvement, laryngo-tracheobronchial stenosis, pulmonary involvement by radiography or CT, ANCA positivity, and renal involvement (proteinuria, hematuria, pauci-immune glomerulonephritis) [6–8]. Considering its 100% mortality rate when left untreated, GPA requires routine glucocorticoid and cyclophosphamide immunosuppressive therapy, which enables 85–100% survival but with a 75% chance of relapse [1, 5].

Given GPA's characteristic sinonasal, airway and lung involvement, CT is generally the preferred imaging modality (Fig. 8) [2]. Indeed, pulmonary symptoms are absent in up to one-third of patients despite abnormal findings at imaging [1]. The most common pulmonary findings are multifocal lung nodules, usually >5, and many of these are >5 mm in diameter, with a random distribution and cavitation in nearly one-fifth, more commonly in larger (>2 cm) masses [1, 2]. Cavity walls might be thick or thin [2]. The second-most common findings, occurring in approximately half of patients, are ground-glass opacities and airspace consolidations [1, 2]. Both "halo" and "reverse halo" appearances have been observed, attributed to hemorrhage around a nodule or organizing pneumonia at the periphery of a hemorrhage, respectively [1]. A mosaic attenuation pattern can also be observed and is thought to reflect altered perfusion caused by vasculitis [2]. Mediastinal lymphadenopathy and pleural effusions are uncommon. Notably, even extensive pulmonary findings including ground-glass opacities and cavitary nodules can resolve or nearly resolve on follow-up [1].

Subglottic, tracheal or bronchial stenosis is reported to have nearly 100% specificity for the diagnosis of GPA and is also effectively demonstrated by CT [1, 2, 8]. On imaging, this is evidenced by smooth or irregular wall thickening with luminal narrowing [1]. Virtual bronchoscopic images reconstructed from source data can be a useful

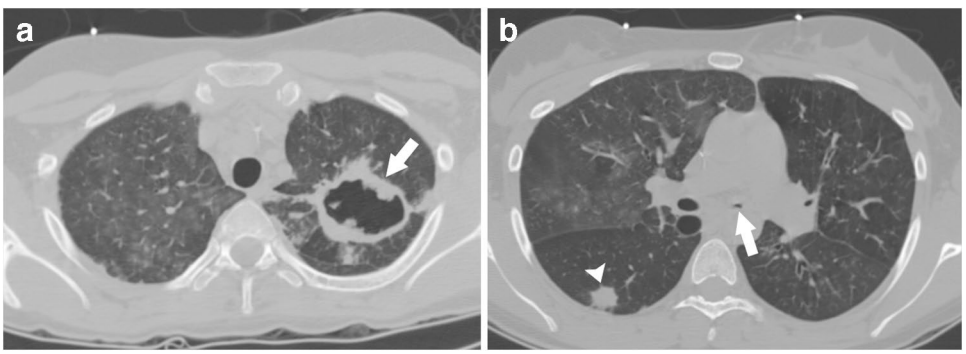

Fig. 8 Granulomatosis with polyangiitis (formerly Wegener granulomatosis). **a** Axial non-contrast lung window CT image in an 18-year-old woman shows a large cavitary mass (*arrow*) in the left apex. **b** More caudal axial CT image from the same exam shows marked narrowing of the left main bronchus (*arrow*) and an additional irregular right lower lobe nodule (*arrowhead*)

adjunct [2]. Airway/lung MRI has not been widely applied in the context of GPA, perhaps the result of local technical limitations or tenuous patient status. Nevertheless, its importance is likely to increase in future years given ongoing advances such as UTE/ZTE acquisitions rivaling CT, potentially providing radiation-free follow-up in people with this lifelong disease [14, 49, 50].

Eosinophilic granulomatosis with polyangiitis

Eosinophilic granulomatosis with polyangiitis (EGPA), formerly known as Churg–Strauss syndrome, is a necrotizing granulomatous vasculitis with a predilection for small- to medium-size vessels [2]. Eosinophilic vessel inflammation and peripheral eosinophilia are unique features of this disease, as implied by its name [51]. ANCA positivity is also frequently seen when concurrent glomerulonephritis is present [2]. The exact pathogenesis of EGPA remains unclear, although inappropriate Th2 activation and IL-4, IL-5 and IL-13 expression are implicated, triggering an allergic-like response with progressive immune dysregulation [5].

The demographics of EGPA are not well understood because of a paucity of cases across all age groups. In adults, the prevalence of EGPA is estimated at 10.7–17.8 per million, while the annual incidence is estimated at 0.9–2.4 per million. Reliable data in children are not available [51]. In keeping with the allergic/immune hypothesis, prodromal symptoms lasting several years are classically initially present, including chronic sinusitis and severe asthma, followed by multi-organ involvement including the lungs, gastrointestinal tract, heart, skin and peripheral nerves [5]. Renal involvement has also been described [52].

No pediatric-specific EGPA criteria are available; instead, often used are the adult American College of Rheumatology criteria indicating that at least four of the following six features should be present: asthma, peripheral eosinophilia >10%, mono- or polyneuropathy, non-static pulmonary airspace disease, sinus abnormalities and biopsy-proven extravascular eosinophils [51, 53]. The slightly older but more parsimonious Lanham criteria are also popular, requiring all three of the following to be present: asthma, peak peripheral eosinophil count >1.5 million, and systemic vasculitis involving at least two organs [51, 54]. Glucocorticoids are the mainstay of treatment with generally good response, although newer immunosuppressants such as mepolizumab and rituximab show promise [51].

The characteristic radiographic pulmonary findings of EGPA are bilateral, non-segmental, fluctuating airspace opacities in a random distribution. On CT, these appear as areas of ground glass or consolidation, often bilateral with a symmetrical peripheral distribution, accompanied by septal thickening in approximately half of cases [2]. Cardiac MRI has been shown to outperform other diagnostic methods in demonstrating early cardiac involvement of EGPA, arguing for its routine use [55]. Subendocardial late gadolinium enhancement is a distinct feature that is attributed to non-ischemic eosinophilic subendocardial fibrosis vs. ischemic scar from an unrecognized myocardial infarction (Fig. 9) [56]. Other findings might include wall motion abnormalities, increased native T1, increased myocardial extracellular volume, increased extracellular matrix mass, and non-ischemic late gadolinium enhancement (e.g., mesocardial, epicardial, right ventricular insertion site or a combination) [55, 56].

Microscopic polyangiitis

Microscopic polyangiitis is an ANCA-associated necrotizing vasculitis with a predilection for small vessels [2]. Autoantibodies are usually directed against myeloperoxidase (MPO-ANCA) rather than proteinase 3 (PR3-ANCA) [2, 57]. As

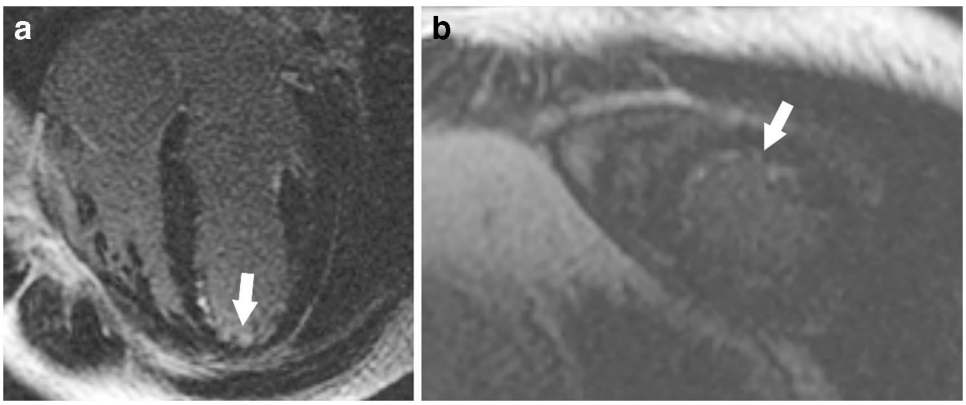

Fig. 9 Eosinophilic granulomatosis with polyangiitis (formerly Churg–Strauss syndrome). **a, b** Four-chamber (**a**) and short-axis (**b**) late-gadolinium-enhancement MR images in a 16-year-old boy using magnitude inversion recovery technique and a spoiled gradient echo readout show abnormal, near-circumferential subendocardial late gadolinium enhancement (*arrow*) at the left ventricular apex, compatible with the eosinophilic pattern of fibrosis observed in this disorder

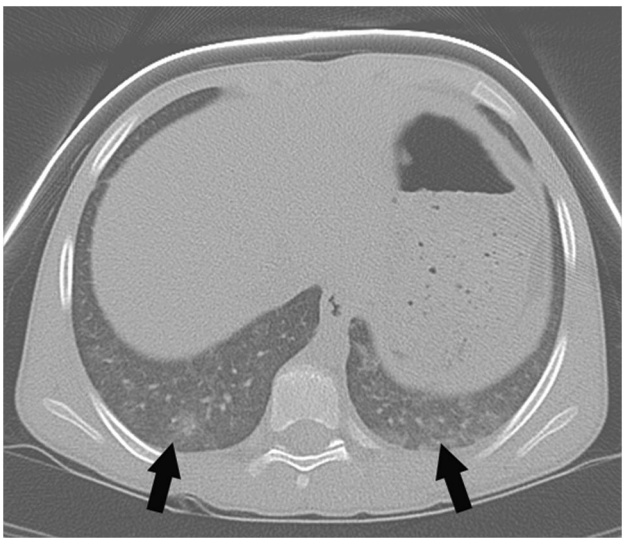

Fig. 10 Microscopic polyangiitis. Axial non-contrast lung window CT image in a 10-year-old girl shows predominantly peripheral ground-glass opacities (*arrows*) at the lung bases

in other ANCA-associated vasculitides, excessive neutrophil activation results in abnormally increased cytokines, which trigger release of lytic enzymes and reactive oxygenic-specific radicals. These pathways then lead to production of neutrophil extracellular traps, which are associated with angiopathy [58].

Epidemiological data on pediatric microscopic polyangiitis are limited; in one Swedish study, the annual incidence was estimated at 1.4 cases per million [58, 59]. Patients often present with nonspecific constitutional symptoms such as weight loss, fever, arthralgias and myalgias, leading to delayed diagnosis [58]. Lung and kidney involvement (pulmonary-renal syndrome) is characteristic [2, 58]. Pulmonary symptoms might include cough, chest pain, hemoptysis or anemia (secondary to pulmonary hemorrhage caused by pulmonary capillaritis), while renal disease might manifest as hypertension, hematuria or proteinuria [2, 57, 58]. No well-defined classification criteria exist in children or adults [58, 60]. Treatments include high-dose glucocorticoids and cyclophosphamide [60].

Lung findings are best appreciated on CT and include ground-glass opacities (reflecting alveolar hemorrhage as well as chronic inflammation and fibrosis), interlobular septal thickening, reticulation, consolidation and honeycombing; findings are more often symmetrical with a peripheral, lower-lung predominance (Fig. 10) [57]. The presence of subpleural sparing, in which the lung periphery abutting the pleura (≤1 cm) is not involved, supports a pulmonary hemorrhage pattern [61]. Unlike in GPA, the upper airway in microscopic polyangiitis is usually not involved, although there can be bronchial wall thickening or bronchiectasis [2, 57]. Lung findings, except for honeycombing reflecting late-stage fibrosis, can partially or completely resolve with successful treatment [57].

Other vasculitis

Behçet disease

Behçet disease is an immune-mediated vasculitis affecting both arteries and veins of any size (small, medium or large) and thus is also termed a variable vessel vasculitis [2, 9]. The pathogenesis remains unclear, although an autoinflammatory response involving activation of neutrophils and monocytes and subsequently IL-1 is implicated [62]. Although Behçet usually manifests after 20 years of age, children can be affected [2]. Characteristic clinical features include recurrent oral or genital aphthous ulcers, skin lesions, uveitis and cardiovascular complications [2, 9]. Treatments include glucocorticoids as well as immunosuppressive and biologic agents targeting proinflammatory cytokines [62].

The pulmonary arteries are a characteristic site of vascular involvement in Behçet and can be readily evaluated by CT or MRI. In particular, pulmonary artery aneurysms can develop, and these can rupture and lead to massive hemorrhage or thrombose and cause lung infarction [2]. In fact, there should be high suspicion for Behçet disease in a child with a pulmonary artery aneurysm and unexplained vasculitis [2, 63]. Although veins are overall more affected than are arteries, additional sites of cardiothoracic involvement might include the aorta and coronary arteries (Fig. 11) [64].

Other causes of vasculitis

Numerous disorders can secondarily cause vasculitis in children, usually with small-vessel predominance and likely related to a particular antigen/disease triggering overall increased vascular inflammation. Etiologies include systemic autoimmune and connective tissue diseases, infections, medications and malignancies [1, 2]. Successful treatment of the underlying stimulus/disease usually should be expected cause improvement in the vasculitic findings [1].

Vasculitis mimics

A variety of other diseases can cause arterial stenosis in children resembling that of vasculitis, especially the large-vessel type [1]. These include fibromuscular dysplasia,

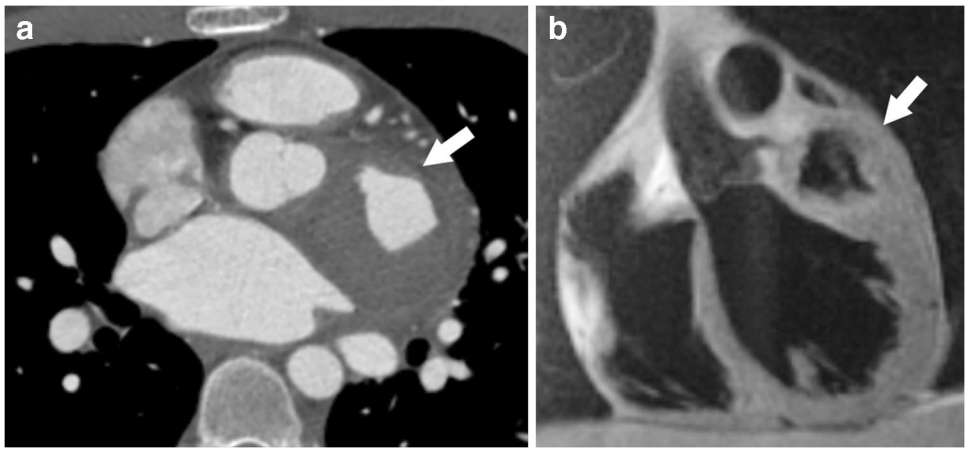

Fig. 11 Behçet disease in a 15-year-old boy. **a, b** Axial contrast-enhanced electrocardiographic (ECG)-gated coronary CT angiogram (**a**) and coronal T2-weighted double inversion recovery black-blood non-contrast MR image (**b**) show a large, partially thrombosed aneurysm (*arrow*) of the left circumflex coronary artery

neurofibromatosis 1, William syndrome, Alagille syndrome, mid-aortic syndrome and prior radiation therapy [1, 65]. However, unlike in vasculitis, vessel wall edema, thickening, enhancement and FDG avidity should be absent in mimics [1]. Given its ability to demonstrate both active vascular inflammation (edema, enhancement, FDG avidity) and fibrous changes (stenosis, wall thickening), hybrid PET/MRI is an attractive option if available and the differential diagnosis is broad, including both vasculitic and non-vasculitic etiologies (Fig. 12) [33, 66].

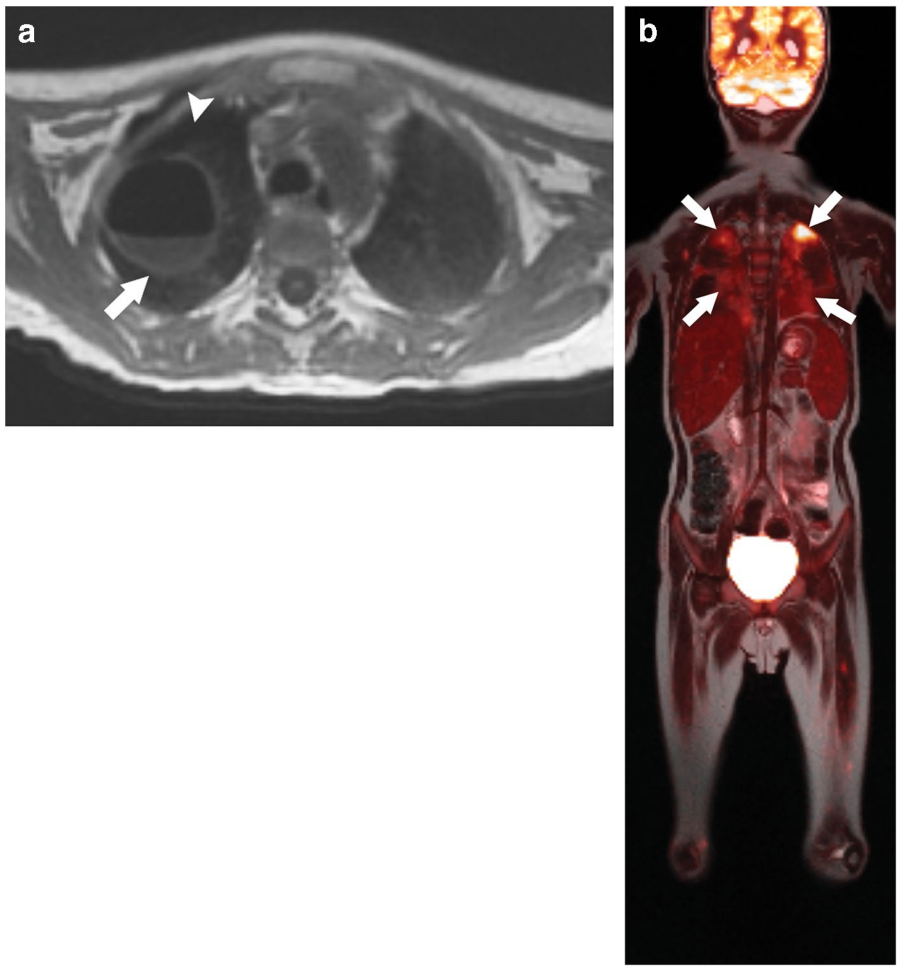

Fig. 12 Juvenile dermatomyositis and cytomegalovirus pneumonia with question of vasculitis in a 5-year-old boy. **a** Axial non-contrast T1-weighted ultrashort echo time (UTE) MR image shows a large cavitary pneumonia (*arrow*) at the right lung apex, along with a small pneumothorax (*arrowhead*). **b** Coronal fused [F-18]2-fluoro-2-deoxyglucose (^{18}F-FDG) positron emission tomography (PET)/T2-weighted MR image shows intense radiotracer avidity in the lungs (*arrows*), compatible with ongoing active infection/inflammation. However, there is no abnormal uptake in the large vasculature. These findings argue against a superimposed active large-vessel vasculitis, although they do not exclude small-vessel disease

Conclusion

Chest involvement is common to many childhood vasculitides, which nonetheless remain rare and enigmatic with often insidious symptoms and limited pediatric-specific clinical criteria. As such, imaging, particularly CT, MRI and PET, has garnered increasing importance in the diagnosis and surveillance of such disorders. The most appropriate imaging modality is dependent on the underlying disease process, institutional experience and patient factors. In general, MRI, with its improved utility for identifying active inflammation, is preferable for large-vessel vasculitis, although CT is a reasonable option. CT is likely to be preferred for disorders with significant coronary (e.g., Kawasaki) or lung (e.g., GPA) involvement, although MRI is desirable because of its absence of ionizing radiation and its increasingly effective newer methods (e.g., UTE/ZTE). PET provides a surrogate for disease activity, although the added prognostic value is not entirely understood. Finally, hybrid PET/MRI is a promising one-stop alternative when the differential diagnosis is broad and includes both vasculitis and non-vasculitis mimics. With ongoing advances in imaging, more comprehensive understanding of the pediatric vasculitides, along with early recognition of disease activity and remission, is likely to increase.

Acknowledgments Portions of this work were presented at the 14th Society for Pediatric Radiology (SPR) Advanced Symposium on Pediatric Cardiovasular Imaging (2018), the 104th Radiological Society of North America (RSNA) Scientific Assembly and Annual Meeting (2018), and the SPR 2021 Thoracic Imaging Course.

Declarations

Conflicts of interest None

References

1. Khanna G, Sargar K, Baszis KW (2015) Pediatric vasculitis: recognizing multisystemic manifestations at body imaging. Radiographics 35:849–865
2. Soliman M, Laxer R, Manson D et al (2015) Imaging of systemic vasculitis in childhood. Pediatr Radiol 45:1110–1125
3. Gardner-Medwin JM, Dolezalova P, Cummins C, Southwood TR (2002) Incidence of Henoch-Schönlein purpura, Kawasaki disease, and rare vasculitides in children of different ethnic origins. Lancet 360:1197–1120
4. Barut K, Sahin S, Kasapcopur O (2016) Pediatric vasculitis. Curr Opin Rheumatol 28:29–38
5. Schnabel A, Hedrich CM (2019) Childhood vasculitis. Front Pediatr 6:421
6. Ozen S, Ruperto N, Dillon MJ et al (2006) EULAR/PReS endorsed consensus criteria for the classification of childhood vasculitides. Ann Rheum Dis 65:936–941
7. Ruperto N, Ozen S, Pistorio A et al (2010) EULAR/PRINTO/PRES criteria for Henoch-Schönlein purpura, childhood polyarteritis nodosa, childhood Wegener granulomatosis and childhood Takayasu arteritis: Ankara 2008. Part I: overall methodology and clinical characterization. Ann Rheum Dis 69:790–797
8. Ozen S, Pistorio A, Iusan SM et al (2010) EULAR/PRINTO/PRES criteria for Henoch-Schönlein purpura, childhood polyarteritis nodosa, childhood Wegener granulomatosis and childhood Takayasu arteritis: Ankara 2008. Part II: final classification criteria. Ann Rheum Dis 69:798–806
9. Jennette JC, Falk RJ, Bacon PA et al (2013) 2012 revised international Chapel Hill consensus conference nomenclature of vasculitides. Arthritis Rheum 65:1–11
10. Schmidt WA, Nielsen BD (2020) Imaging in large-vessel vasculitis. Best Pract Res Clin Rheumatol 34:101589
11. Guggenberger KV, Bley TA (2020) Imaging in vasculitis. Curr Rheumatol Rep 22:34
12. Siegel MJ, Ramirez-Giraldo JC (2019) Dual-energy CT in children: imaging algorithms and clinical applications. Radiology 291:286–297
13. Tesche C, De Cecco CN, Albrecht MH et al (2017) Coronary CT angiography-derived fractional flow reserve. Radiology 285:17–33
14. Zucker EJ, Cheng JY, Haldipur A et al (2018) Free-breathing pediatric chest MRI: performance of self-navigated golden-angle ordered conical ultrashort echo time acquisition. J Magn Reson Imaging 47:200–209
15. Sandberg JK, Young VA, Yuan J et al (2021) Zero echo time pediatric musculoskeletal magnetic resonance imaging: initial experience. Pediatr Radiol 51:2549–2560
16. Kamada H, Ota H, Aoki T et al (2019) 4D-flow MRI assessment of blood flow before and after endovascular intervention in a patient with pulmonary hypertension due to isolated pulmonary artery involvement in large vessel vasculitis. Radiol Case Rep 15:190–194
17. Kemna MJ, Vandergheynst F, Vöö S et al (2015) Positron emission tomography scanning in anti-neutrophil cytoplasmic antibodies-associated vasculitis. Medicine 94:e747
18. Muratore F, Pipitone N, Salvarani C, Schmidt WA (2016) Imaging of vasculitis: state of the art. Best Pract Res Clin Rheumatol 30:688–706
19. Schmidt WA (2013) Imaging in vasculitis. Best Pract Res Clin Rheumatol 27:107–118
20. Aeschlimann FA, Twilt M, Yeung RSM (2020) Childhood-onset Takayasu arteritis. Eur J Rheumatol 7:S58–S66
21. Wadowski B, Chadha T, Wen AY (2017) A 15-year-old with aphasia and right hemiparesis. J Pediatr Intensive Care 6:221–224
22. Di Santo M, Stelmaszewski EV, Villa A (2018) Takayasu arteritis in paediatrics. Cardiol Young 28:354–361
23. Zhang N, Pan L, Liu J et al (2022) Comparison of different thoracic aortic wall characteristics for assessment of disease activity in Takayasu arteritis: a quantitative study with 3.0 T magnetic resonance imaging. Rev Cardiovasc Med 23:92
24. Tso E, Flamm SD, White RD et al (2002) Takayasu arteritis: utility and limitations of magnetic resonance imaging in diagnosis and treatment. Arthritis Rheum 46:1634–1642
25. Choe YH, Han BK, Koh EM et al (2000) Takayasu's arteritis: assessment of disease activity with contrast-enhanced MR imaging. AJR Am J Roentgenol 175:505–511
26. Kato Y, Terashima M, Ohigashi H et al (2015) Vessel wall inflammation of Takayasu arteritis detected by contrast-enhanced magnetic resonance imaging: association with disease distribution and activity. PLoS One 10:e0145855
27. Yang H, Lv P, Zhang R et al (2021) Detection of mural inflammation with low b-value diffusion-weighted imaging in patients with active Takayasu arteritis. Eur Radiol 31:6666–6675

28. Papa M, De Cobelli F, Baldissera E et al (2012) Takayasu arteritis: intravascular contrast medium for MR angiography in the evaluation of disease activity. AJR Am J Roentgenol 198:W279–W284
29. Runge VM, Heverhagen JT (2018) Advocating the development of next-generation high-relaxivity gadolinium chelates for clinical magnetic resonance. Investig Radiol 53:381–389
30. Vasanawala SS, Nguyen KL, Hope MD et al (2016) Safety and technique of ferumoxytol administration for MRI. Magn Reson Med 75:2107–2111
31. Hedgire S, Krebill C, Wojtkiewicz GR et al (2018) Ultrasmall superparamagnetic iron oxide nanoparticle uptake as noninvasive marker of aortic wall inflammation on MRI: proof of concept study. Br J Radiol 91:20180461
32. Soussan M, Nicolas P, Schramm C et al (2015) Management of large-vessel vasculitis with FDG-PET: a systematic literature review and meta-analysis. Medicine 94:e622
33. Laurent C, Ricard L, Fain O et al (2019) PET/MRI in large-vessel vasculitis: clinical value for diagnosis and assessment of disease activity. Sci Rep 9:12388
34. Rife E, Gedalia A (2020) Kawasaki disease: an update. Curr Rheumatol Rep 22:75
35. Feldstein LR, Rose EB, Horwitz SM et al (2020) Multisystem inflammatory syndrome in U.S. children and adolescents. N Engl J Med 383:334–346
36. Nakra NA, Blumberg DA, Herrera-Guerra A, Lakshminrusimha S (2020) Multi-system inflammatory syndrome in children (MIS-C) following SARS-CoV-2 infection: review of clinical presentation, hypothetical pathogenesis, and proposed management. Children 7:69
37. Kitamura S, Tsuda E (2019) Significance of coronary revascularization for coronary-artery obstructive lesions due to Kawasaki disease. Children 6:16
38. McCrindle BW, Rowley AH, Newburger JW et al (2017) Diagnosis, treatment, and long-term management of Kawasaki disease: a scientific statement for health professionals from the American Heart Association. Circulation 135:e927–e999
39. Lee MS, Liu YC, Tsai CC et al (2021) Similarities and differences between COVID-19-related multisystem inflammatory syndrome in children and Kawasaki disease. Front Pediatr 9:640118
40. van Stijn D, Planken N, Kuipers I, Kuijpers T (2021) CT angiography or cardiac MRI for detection of coronary artery aneurysms in Kawasaki disease. Front Pediatr 9:630462
41. Goo HW (2015) Coronary artery imaging in children. Korean J Radiol 16:239–250
42. Dietz SM, Tacke CE, Kuipers IM et al (2015) Cardiovascular imaging in children and adults following Kawasaki disease. Insights Imaging 6:697–705
43. Tacke CE, Kuipers IM, Groenink M et al (2011) Cardiac magnetic resonance imaging for noninvasive assessment of cardiovascular disease during the follow-up of patients with Kawasaki disease. Circ Cardiovasc Imaging 4:712–720
44. Jin KN, De Cecco CN, Caruso D et al (2016) Myocardial perfusion imaging with dual energy CT. Eur J Radiol 85:1914–1921
45. Goo HW (2017) Myocardial delayed-enhancement CT: initial experience in children and young adults. Pediatr Radiol 47:1452–1462
46. Rajiah P, Cummings KW, Williamson E, Young PM (2022) CT fractional flow reserve: a practical guide to application, interpretation, and problem solving. Radiographics 42:340–358
47. Rehani C, Nelson JS (2021) Coronary artery aneurysms as a feature of granulomatosis with polyangiitis. Pediatrics 147:e20200932
48. Lee PY, Adil EA, Irace AL et al (2017) The presentation and management of granulomatosis with polyangiitis (Wegener's granulomatosis) in the pediatric airway. Laryngoscope 127:233–240
49. Liszewski MC, Ciet P, Lee EY (2019) MR imaging of lungs and airways in children: past and present. Magn Reson Imaging Clin N Am 27:201–225
50. Sodhi KS, Bhatia A, Lee EY (2021) Prospective evaluation of free-breathing fast T2-weighted MultiVane XD sequence at 3-T MRI for large airway assessment in pediatric patients. AJR Am J Roentgenol 216:1074–1080
51. Furuta S, Iwamoto T, Nakajima H (2019) Update on eosinophilic granulomatosis with polyangiitis. Allergol Int 68:430–436
52. Oldan J, McCauley R, Pilichowska M et al (2011) Unusual finding in pediatric Churg-Strauss: renal lesions on CT. Pediatr Radiol 41:1065–1068
53. Masi AT, Hunder GG, Lie J et al (1990) The American College of Rheumatology 1990 criteria for the classification of Churg-Strauss syndrome (allergic granulomatosis and angiitis). Arthritis Rheum 33:1094–1100
54. Lanham JG, Elkon KB, Pusey CD, Hughes GR (1984) Systemic vasculitis with asthma and eosinophilia: a clinical approach to the Churg-Strauss syndrome. Medicine 63:65–81
55. Sridharan S, Nanthakumaran S, Somagutta MR et al (2020) The critical role of cardiac magnetic resonance imaging in evaluating patients with eosinophilic granulomatosis with polyangiitis. Cureus 12:e10279
56. Lagan J, Naish JH, Fortune C et al (2021) Myocardial involvement in eosinophilic granulomatosis with polyangiitis evaluated with cardiopulmonary magnetic resonance. Int J Cardiovasc Imaging 37:1371–1381
57. Alba MA, Flores-Suárez LF, Henderson AG et al (2017) Interstital [sic] lung disease in ANCA vasculitis. Autoimmun Rev 16:722–729
58. Jariwala M, Laxer RM (2020) Childhood GPA, EGPA, and MPA. Clin Immunol 211:108325
59. Mossberg M, Segelmark M, Kahn R et al (2018) Epidemiology of primary systemic vasculitis in children: a population-based study from southern Sweden. Scand J Rheumatol 47:295–302
60. Calatroni M, Oliva E, Gianfreda D et al (2017) ANCA-associated vasculitis in childhood: recent advances. Ital J Pediatr 43:46
61. Chong WH, Saha BK, Austin A, Chopra A (2021) The significance of subpleural sparing in CT chest: a state-of-the-art review. Am J Med Sci 361:427–435
62. Alibaz-Oner F, Direskeneli H (2021) Advances in the treatment of Behcet's disease. Curr Rheumatol Rep 23:47
63. Kokturk A (2012) Clinical and pathological manifestations with differential diagnosis in Behçet's disease. Pathol Res Int 2012:69039
64. Cevik C, Otahbachi M, Nugent K, Jenkins LA (2009) Coronary artery aneurysms in Behçet's disease. Cardiovasc Revasc Med 10:128–129
65. Maningding E, Kermani TA (2021) Mimics of vasculitis. Rheumatology 60:34–47
66. Pelletier-Galarneau M, Ruddy TD (2019) PET/CT for diagnosis and management of large-vessel vasculitis. Curr Cardiol Rep 21:34

Publisher's note Springer Nature remains neutral with regard to jurisdictional claims in published maps and institutional affiliations.